IEEE Access
Multidisciplinary | Rapid Review | Open Access Journal

Received May 25, 2018, accepted June 28, 2018, date of publication July 5, 2018, date of current version July 30, 2018.

Digital Object Identifier 10.1109/ACCESS.2018.2853145

Attitude Control of Aircraft Using Only Synthetic Jet Actuators When Stall Occurs

CHUNZHI LI, TINGTING ZHANG, AND JIANYING YANG

State Key Laboratory for Turbulence and Complex Systems, Department of Mechanics and Engineering Science, College of Engineering, Peking University, Beijing 100871, China

Corresponding author: Jianying Yang (yjy@pku.edu.cn).

This work was supported by the National Natural Science Key Foundation of China under Grant 11332001.

ABSTRACT This paper proposes a novel active flow control method for a special aircraft, that using only synthetic jet actuators (SJAs) to achieve pitch-roll-yaw attitude control at a high angle of attack when the stall occurs. The special aircraft goes without traditional aileron, elevator, or vertical stabilizer. As the first step, the model of the aircraft is built and the relation between the velocity amplitude of SJAs and the moments provided by SJAs are derived. The next step, to solve the problem that parameter uncertainties, unmodeled dynamics, and unknown external disturbances exist in the aircraft system, a sliding mode controller base on extended state observer (ESO) is designed. The parameter uncertainties, unmodeled dynamics, and unknown external disturbances are regarded as the compound interference of the system, which is estimated by the ESO and compensated in real time. Finally, the effectiveness of the proposed controller is verified through the numerical simulations. Simulation results show that the proposed control method is feasible and effective to solve the difficult problem of attitude control when the stall occurs.

INDEX TERMS Synthetic jet actuators, high-angle-of-attack, attitude control, extended state observer.

NOMENCLATURE

$\mathbf{A}_{SJ}$	= the VASJAs [m/s]
b_1	= the distance between aerodynamic center of tails and center of mass, 1000 [mm]
b_2	= the distance between aerodynamic center of wings and center of mass, 500 [mm]
C	= chord of airfoil, 300 [mm]
$\mathbf{Cl}_{SJ}$	= the increment of lift coefficient caused by SJAs
$\mathbf{Cd}_{SJ}$	= the decrement of drag coefficient caused by SJAs
g	= gravity acceleration [m/s^2]
L	= wing span of airfoil, 2000 [mm]
L_r	= reference length, 2000 [mm]
m	= aircraft mass [kg]
m_x^*, m_y^*, m_z^*	= atmospheric moment coefficients
$\mathbf{M}_{SJ}$	= the control moments provided by SJAs [N·m]
I_x, I_y, I_z, I_{xz}	= moments of inertia [kg· m^2]
O	= the mass center
p	= roll rate [rad/s]
q	= pitch rate [rad/s]
$\bar{q}$	= dynamic pressure, $0.5\rho U_\infty^2$
r	= yaw rate, rad/s
Re	= Reynolds number based on C and U_∞, $Re \approx 6 \times 10^5$
S_r	= reference area, 0.6 [m^2]
U_∞	= freestream velocity, 30 [m/s]
u, v, w	= speeds of aircraft in body frame, [m/s]
$\mathbf{V}$	= SJAs' excitation voltage [Volts]
x, y, z	= positions of aircraft in earth frame [m]
α	= angle of attack [deg]
ϕ	= roll angle [rad]
θ	= pitch angle [rad]
θ_1	= dihedral angle, 0.3 [rad]
ψ	= yaw angle [rad]
ρ	= air density, 1.225 [kg/m^3]

I. INTRODUCTION

A stall is a condition in aviation and aerodynamics wherein the AOA increases beyond a certain point such that lift begins to decrease. At the onset of the stall, the air near the leading edge of the wing separates from the wing surface, which can cause the plane to crash. Fortunately, flow control using SJAs has been shown [1]–[4] to effectively reattach the boundary layer and at the same time reduce the wing's frictional drag. The SJAs originated from the idea of acoustic streaming [5]. Currently, most SJAs make use of piezoelectrically driven

2169-3536 © 2018 IEEE. Translations and content mining are permitted for academic research only.
Personal use is also permitted, but republication/redistribution requires IEEE permission.
See http://www.ieee.org/publications_standards/publications/rights/index.html for more information.

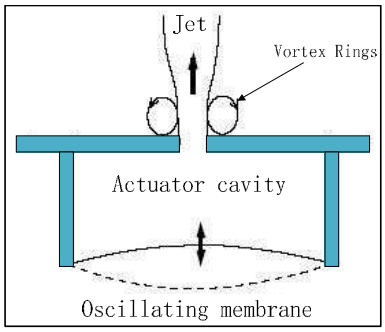

FIGURE 1. Synthetic jet actuator [2].

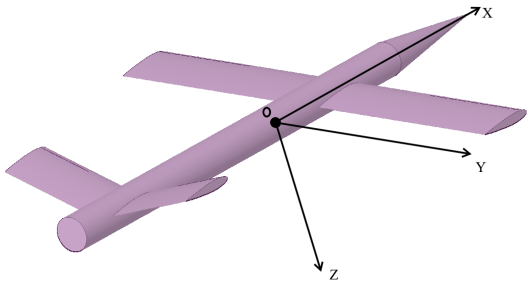

FIGURE 2. Sketch representation of a scale model aircraft.

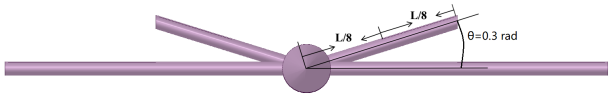

FIGURE 3. Front view of the aircraft.

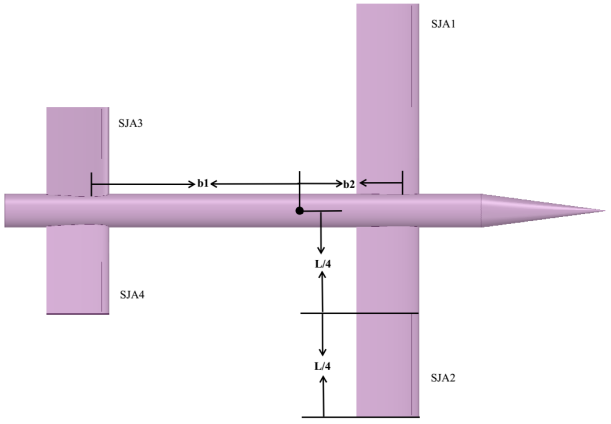

FIGURE 4. Top view of the fuselage.

diaphragms to produce a synthetic jet. As shown in Fig. 1, the SJA is constructed with a rigid sidewall cavity, an aperture and a diaphragm (on the opposite surface). When the oscillating membrane vibrates at a certain frequency [6], the fluid from the surroundings is expelled (blowing stage) and ingested (suction stage) through the aperture. Therefore, jets generated by SJAs [7]–[9] have zero net mass but non-zero momentum. The oscillatory motion of the SJA creates a coherent vortex ring which delays flow separation and provides good control effect with zero net mass flux [10]–[12]. The advantages of using SJAs include compact structure, low cost, quick dynamic response and simple and convenient operation. Those make SJA a very efficient active flow control device.

There are many researches focusing on the SJAs' effect on aerodynamic parameters of the airfoil while few of them have applied SJAs into flight control. Experiments conducted by Neuburger and Wygnanski [13], Bar-Sever [14] and Seifert *et al.* [11], effectively demonstrated that air separation can be delayed and even be fully prevented by introducing fierce oscillations in the region of incipient separation. Different active mechanical devices embedded in the boundary layer were used in these experiments. Margalit *et al.* and Seifert *et al.* [15], [16] studied the theory of delta wing stall roll control using segmented piezoelectric fluidic actuators. Li and Yang [17], [18] applied SJAs to rolling control for a straight airfoil at high AOA. Ciuryla *et al.* [19] integrated SJAs with the aileron, elevator and rudder. It turned out that the velocity change rate of Cessna's body can be taken control at low AOA by this integrated control system.

This present study focuses on applying only SJAs into pitch-roll-yaw attitude control of a special aircraft at high AOA. The aircraft occupies the following three characteristics. The first one is that it does not have the traditional control surfaces such as aileron, elevator and rudder. The second is the aircraft has no vertical stabilizer. We get remove the vertical stabilizer because it is heavy and usually its AOA is small then the effect of the SJAs is not significant. To maintain static stability, a horizontal stabilizer with dihedral angle is designed as shown in Fig. 2, Fig. 3 and Fig. 4. The third is that there are parameter uncertainties, unmodeled dynamics and external disturbances in the aircraft system. They were compensated by the ESO, as mentioned in [20] and [21]. It turned out to have high efficiency in accomplishing the nonlinear dynamic estimation [22]. Xia *et al.* [23] have applied the ESO to control a missile systems, then they achieved attitude tracking of a rigid spacecraft via ESO [24]. Considering the above characteristics of the aircraft, we design a relatively robust and practical control method based on ESO. The pitch-roll-yaw attitude control, at high AOA, is realized by solely using SJAs.

A preliminary conference version of this paper appeared in Li and Yang [25]. The main improvement with respect to this earlier work is the more reasonable and accurate calculation of data and more effective and robust control method. The approximate relation between voltage and VASJAs is also considered.

II. MODEL

When the aircraft is under the condition of stall, its control surfaces almost disable to control aircraft effectively. In order to achieve effective flight control, we place the SJAs on the upper surface of the wings and horizontal stabilizers instead of the traditional aileron and elevator, as shown in Fig. 2,

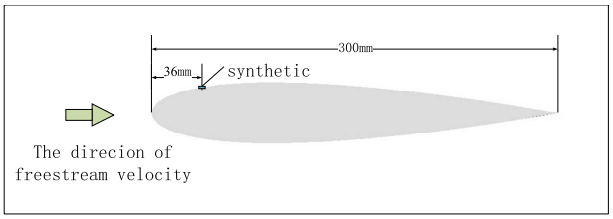

FIGURE 5. Side view of the airfoil.

Fig. 4 and Fig. 5. It is also an innovation of this article that the dihedral angle of horizontal stabilizer works cooperatively with SJAs to realize pitch-roll-yaw attitude control. The horizontal stabilizers have a dihedral angle $\theta_1 = 0.3$ [rad]. Both the wings' and horizontal stabilizers' airfoil profile are NACA0015. The coordinate origin of body axes is set at the mass center of aircraft, and the directions of each axis are shown in Fig. 2.

A. THE RELATION BETWEEN MOMENTS AND VASJAS

The airfoil's chord length $C = 0.3$ [m] and its characteristic frequency $f = 100$ [Hz] when the freestream velocity $U_\infty = 30$ [m/s]. In our previous work [18], we found that the lift coefficient improved by SJAs is optimal when the follow conditions are met: (1) The frequency of SJAs is equal to the characteristic frequency of the airfoil, that is, $f = 100$ [Hz]; (2) SJAs exit angle is set to 45 [deg]; (3) The SJAs is located 12% of the chord of the airfoil. So the placement of the SJAs according to the above conditions is given as shown in Fig. 4 and Fig. 5. From Fig. 6 we can find that the stall occurs when wings' AOA is greater than 15 [deg] and the control efficiency of the SJAs reaches best when wings' AOA is about 19 [deg].

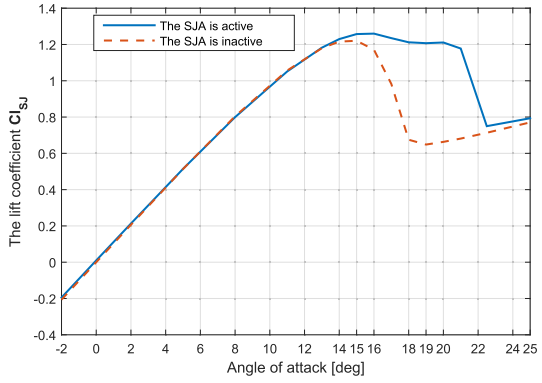

FIGURE 6. The lift coefficient vs. AOA.

Based on the above conditions, as long as the VASJAs is less than the freestream velocity, the increase of airfoil's lift coefficient is quadratic to VASJAs as shown in Fig. 7. The functional relation between VASJAs $\mathbf{A}_{SJ} \in R^4$ and the increase of airfoil's lifting coefficient $\mathbf{Cl}_{SJ} \in R^4$ as the following equation (1)

$$\begin{aligned} Cl_{SJ_i} &= f_{Cl_{SJ}}(A_{SJ_i}) \\ &= 0.0000392A_{SJ_i}^2 + 0.0003291A_{SJ_i}. \end{aligned} \tag{1}$$

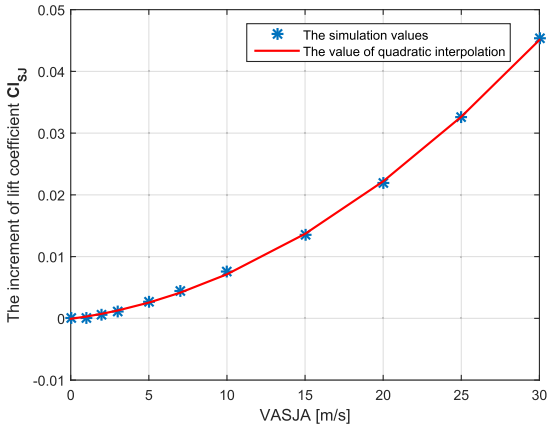

FIGURE 7. Increment of lift coefficient vs. VASJAs.

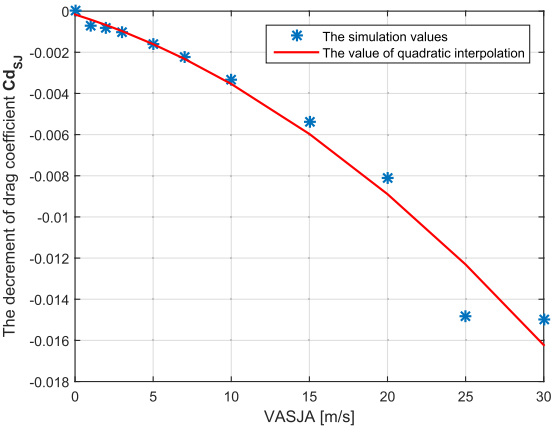

FIGURE 8. Decrement of drag coefficient vs. VASJAs.

where $A_{SJ_i}, i \in \{1, 2, 3, 4\}$ are the components of the VASJAs. As shown in Fig. 8, the decrease of airfoil's drag coefficient $\mathbf{Cd}_{SJ} \in R^4$ is quadratic to the VASJAs, too. Their functional relation is described by equation (2)

$$\begin{aligned} Cd_{jet_i} &= f_{Cd_{jet}}(A_{SJ_i}) \\ &= -0.0000099A_{SJ_i}^2 - 0.0002386A_{SJ_i}, \end{aligned} \tag{2}$$

where $i \in \{1, 2, 3, 4\}$.

From Fig. 9 [26], we can find that there is an approximate relation between the VASJAs and SJAs' excitation voltage $\mathbf{V} \in R^4$

$$\begin{aligned} A_{SJ_i} &= f_A(V_i) \\ &\approx 0.67V_i, V_i < 70[Volts], i \in \{1, 2, 3, 4\} \end{aligned} \tag{3}$$

B. NONLINEAR AIRCRAFT MODEL WITH SJAS

Euler angle is used to describe the aircraft's rotation with respect to the earth frame and the following equations can be obtained:

$$\begin{bmatrix} \dot{\phi} \\ \dot{\theta} \\ \dot{\psi} \end{bmatrix} = \begin{bmatrix} 1 & \sin\phi\tan\theta & \cos\phi\tan\theta \\ 0 & \cos\phi & \sin\phi \\ 0 & \sin\phi\sec\theta & \cos\phi\sec\theta \end{bmatrix} \begin{bmatrix} p \\ q \\ r \end{bmatrix} \tag{4}$$

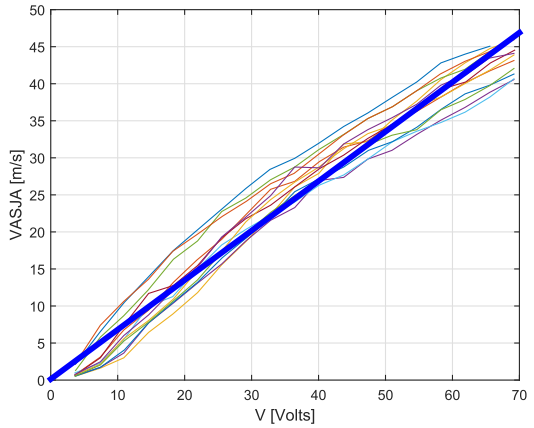

FIGURE 9. VASJAs vs. the excitation voltage.

As being available in most flight dynamic textbooks, the dynamic model of aircraft can be described by (5), as shown at the bottom of this page.

The rearranged moment inertias are

$$
\begin{aligned}
g_l^p &= \frac{I_z}{(I_{xz}^2 - I_x I_z)}, \quad g_n^p = \frac{I_{xz}}{(I_{xz}^2 - I_x I_z)}, \; g_m^q = \frac{1}{I_y}, \\
g_l^r &= \frac{-I_{xz}}{(I_{xz}^2 - I_x I_z)}, \quad g_n^r = \frac{-I_x}{(I_{xz}^2 - I_x I_z)}, \\
I_{pq}^p &= \frac{I_{xz}(I_x + I_z - I_y)}{I_x I_z - I_{xz}^2}, \\
I_{qr}^p &= \frac{I_z(I_y - I_z) - I_{xz}^2}{I_x I_z - I_{xz}^2}, \\
I_{pp}^q &= -\frac{I_{xz}}{I_y}, \quad I_{rr}^q = \frac{I_{xz}}{I_y}, \; I_{pr}^q = \frac{I_z - I_x}{I_y}, \\
I_{pq}^r &= \frac{I_x(I_x - I_y) + I_{xz}^2}{I_x I_z - I_{xz}^2}, \\
I_{qr}^r &= \frac{I_{xz}(I_y - I_x - I_z)}{I_x I_z - I_{xz}^2}.
\end{aligned}
$$

Translational Dynamics as equations (6) and (7), as shown at the bottom of this page

$$
\begin{bmatrix} \dot{u} \\ \dot{v} \\ \dot{w} \end{bmatrix} = \begin{bmatrix} \frac{1}{m}(F_x - mgS_\theta) - qw + rv \\ \frac{1}{m}\left(F_y + mgC_\theta S_\phi\right) - ru + pw \\ \frac{1}{m}\left(F_z + mgC_\theta C_\phi\right) - pv + qu \end{bmatrix} \tag{6}
$$

where $C_* = \cos(*)$, $S_* = \sin(*)$.

In the aircraft systems the following assumption is considered.

Assumption 1: In the aircraft model equations (4)−(7), only the attitude angle $[\phi, \theta, \psi]^T$, angular velocities $[p, q, r]^T$ and speeds $[u, v, w]^T$ can be measured.

Assumption 2: For simplicity, we consider the pitch angle control under the condition of $-90 < \theta < 90$ [deg].

In order to depict the aircraft model explicitly, we define the states

$$
\mathbf{x_1} = \begin{bmatrix} \phi \\ \theta \\ \psi \end{bmatrix}, \quad \mathbf{x_2} = \begin{bmatrix} p \\ q \\ r \end{bmatrix}, \quad \mathbf{x_3} = \begin{bmatrix} x \\ y \\ z \end{bmatrix}, \quad \mathbf{x_4} = \begin{bmatrix} u \\ v \\ w \end{bmatrix}, \tag{8}
$$

hence, the equations of the nonliner system are as follows

$$
\dot{\mathbf{x}}_1 = f_1(\mathbf{x}_1)\mathbf{x}_2, \tag{9}
$$

$$
\dot{\mathbf{x}}_2 = f_2(\mathbf{x}_1, \mathbf{x}_2, \mathbf{x}_3, \mathbf{x}_4) + B\mathbf{M}_{SJ}, \tag{10}
$$

$$
\dot{\mathbf{x}}_3 = f_3(\mathbf{x_1})\mathbf{x}_4, \tag{11}
$$

$$
\dot{\mathbf{x}}_4 = f_4(\mathbf{x}_1, \mathbf{x}_2, \mathbf{x}_3, \mathbf{x}_4), \tag{12}
$$

where $\mathbf{M}_{SJ} \in R^3$ is the control moments provided by SJAs, the function f_i, $i \in \{1, 2, 3, 4\}$ and matrix B are described as follows

$$
f_1(\mathbf{x}_2) = \begin{bmatrix} 1 & \sin\phi\tan\theta & \cos\phi\tan\theta \\ 0 & \cos\phi & \sin\phi \\ 0 & \sin\phi\sec\theta & \cos\phi\sec\theta \end{bmatrix} \tag{13}
$$

$$
\begin{aligned}
f_2(\mathbf{x}_1, \mathbf{x}_2, \mathbf{x}_3, \mathbf{x}_4) &= \begin{bmatrix} I_{pq}^p pq + I_{qr}^p qr \\ I_{pp}^q p^2 + I_{rr}^q r^2 + I_{pr}^q pr \\ I_{pq}^r pq + I_{qr}^r qr \end{bmatrix} \\
&+ \bar{q}S_r L_r \begin{bmatrix} g_1^p(m_p^\beta \beta + m_{\dot{p}}^p \dot{p} + m_r^p r) \\ g_2^q(m_q^\alpha \alpha + m_q^{\dot{\alpha}} \dot{\alpha} + m_q^q q) \\ g_3^r(m_r^\beta \beta + m_r^{\dot{\beta}} \dot{\beta} + m_r^p p + m_r^r r) \end{bmatrix}
\end{aligned} \tag{14}
$$

$$
f_3(\mathbf{x}_1) = \begin{bmatrix} C_\theta C_\psi & S_\phi S_\theta S_\psi - C_\phi S_\psi & C_\phi S_\theta C_\psi + S_\phi S_\psi \\ C_\theta S_\psi & S_\phi S_\theta S_\psi + C_\phi C_\theta & C_\phi S_\theta S_\psi - S_\phi C_\psi \\ -S_\theta & S_\phi C_\theta & C_\phi C_\theta \end{bmatrix} \tag{15}
$$

$$
f_4(\mathbf{x}_1, \mathbf{x}_2, \mathbf{x}_3, \mathbf{x}_4) = \begin{bmatrix} (F_x - mgS_\theta)/m - qw + rv \\ \left(F_y + mgC_\theta S_\phi\right)/m - ru + pw \\ \left(F_z + mgC_\theta C_\phi\right)/m - pv + qu \end{bmatrix} \tag{16}
$$

$$
\begin{aligned}
\begin{bmatrix} \dot{p} \\ \dot{q} \\ \dot{r} \end{bmatrix} &= \begin{bmatrix} I_{pq}^p pq + I_{qr}^p qr + g_l^p M_x + g_n^p M_z \\ I_{pp}^q p^2 + I_{rr}^q r^2 + I_{pr}^q pr + g_m^q M_y \\ I_{pq}^r pq + I_{qr}^r qr + g_l^r M_x + g_n^r M_z \end{bmatrix} + \bar{q}S_r L_r \begin{bmatrix} g_l^p(m_p^\beta \beta + m_{\dot{p}}^p \dot{p} + m_r^p r) \\ g_m^q(m_q^\alpha \alpha + m_q^{\dot{\alpha}} \dot{\alpha} + m_q^q q) \\ g_n^r(m_r^\beta \beta + m_r^{\dot{\beta}} \dot{\beta} + m_r^p p + m_r^r r) \end{bmatrix}.
\end{aligned} \tag{5}
$$

$$
\begin{bmatrix} \dot{x} \\ \dot{y} \\ \dot{z} \end{bmatrix} = \begin{bmatrix} C_\theta C_\psi & S_\phi S_\theta S_\psi - C_\phi S_\psi & C_\phi S_\theta C_\psi + S_\phi S_\psi \\ C_\theta S_\psi & S_\phi S_\theta S_\psi + C_\phi C_\theta & C_\phi S_\theta S_\psi - S_\phi C_\psi \\ -S_\theta & S_\phi C_\theta & C_\phi C_\theta \end{bmatrix} \begin{bmatrix} u \\ v \\ w \end{bmatrix}. \tag{7}
$$

$$B = \begin{bmatrix} g_1^p & 0 & g_3^p \\ 0 & g_2^q & 0 \\ g_1^r & 0 & g_3^r \end{bmatrix}. \tag{17}$$

It's reasonable to suppose there is an approximate relationship as eqation (18) based on the Fig. 7 and Fig. 8.

$$f_{Cd}(A_{SJ_i}) = -kf_{Cl}(A_{SJ_i}), \tag{18}$$

where $k \approx 0.3$, $0 \leq A_{SJ_i} \leq 30[m/s]$, $i \in \{1, 2, 3, 4\}$.

$\mathbf{F}_W$ is the magnitude of the lift and drag changed by SJAs in the wind frame, it is expressed as below

$$\mathbf{F}_W = M_W \mathbf{Cl}_{SJ}, \tag{19}$$

where $M_W \in R^{3\times4}$ is an approximate conversion matrix from lift coefficient $\mathbf{Cl}_{SJ}$ to lift and drag changed by SJAs. The matrix M_W is expressed as

$$M_W = \frac{1}{4}\bar{q}S_r \begin{bmatrix} -k & -k & -0.5k & -0.5k \\ 0 & 0 & 0.5\sin\theta_1 & -0.5\sin\theta_1 \\ -1 & -1 & -0.5\cos\theta_1 & -0.5\cos\theta_1 \end{bmatrix}, \tag{20}$$

Therefore, the control moment $\mathbf{M}_{SJ} \in R^3$ provided by SJAs has the following form

$$\mathbf{M}_{SJ} = \begin{bmatrix} \sum_{j=1}^{4} Cl_{SJ_j}(l^{2,j}\sum_{i=1}^{3} m_B^{3,i}m_W^{i,j} - l^{3,j}\sum_{i=1}^{3} m_B^{2,i}m_W^{i,j}) \\ \sum_{j=1}^{4} Cl_{SJ_j}(l^{3,j}\sum_{i=1}^{3} m_B^{1,i}m_W^{i,j} - l^{1,j}\sum_{i=1}^{3} m_B^{3,i}m_W^{i,j}) \\ \sum_{j=1}^{4} Cl_{SJ_j}(l^{1,j}\sum_{i=1}^{3} m_B^{3,i}m_W^{i,j} - l^{2,j}\sum_{i=1}^{3} m_B^{2,i}m_W^{i,j}) \end{bmatrix} \tag{21}$$

where the matrix $l \in R^{3\times4}$ represents the distance from the aerodynamic center of SJAs to each body-axis, named arm of force matrix. According to the layout of the SJAs, we can estimate the value of l. For example, from Fig. 2, Fig. 3 and Fig. 4, we can conclude that the $l^{3,1} = l^{3,2} = 0$, $l^{3,3} = l^{3,4} = \delta_3 < 0$. M_B is the transformation matrix from wind frame to body frame which is given as

$$M_B = \begin{bmatrix} \cos\alpha\cos\beta & -\cos\alpha\sin\beta & \sin\alpha \\ \sin\beta & \cos\beta & 0 \\ -\sin\alpha\cos\beta & \sin\alpha\sin\beta & \cos\alpha \end{bmatrix} \tag{22}$$

Hence, the relation between the $\mathbf{M}_{SJ}$ and the $\mathbf{Cl}_{SJ}$ is

$$\mathbf{M}_{SJ} = M_M \mathbf{Cl}_{SJ}, \tag{23}$$

where the components of M_M have the following form

$$\begin{aligned} m_M^{1,j} &= l^{2,j}\sum_{i=1}^{3} m_B^{3,i}m_W^{i,j} - l^{3,j}\sum_{i=1}^{3} m_B^{2,i}m_W^{i,j}, \\ m_M^{2,j} &= l^{3,j}\sum_{i=1}^{3} m_B^{1,i}m_W^{i,j} - l^{1,j}\sum_{i=1}^{3} m_B^{3,i}m_W^{i,j}, \\ m_M^{3,j} &= l^{1,j}\sum_{i=1}^{3} m_B^{3,i}m_W^{i,j} - l^{2,j}\sum_{i=1}^{3} m_B^{2,i}m_W^{i,j}, \end{aligned} \tag{24}$$

where $i \in \{1, 2, 3\}$, $j \in \{1, 2, 3, 4\}$.

Then, take the equation (3) to (23), we get the following equation

$$\mathbf{M}_{SJ} = M_M f_{Cl} \circ f_A(\mathbf{V}). \tag{25}$$

The equation (25) reveals the relation between the excitation voltage of SJAs and the moments provided by SJAs. Therefore, the equation (10) can be rewritten as follows

$$\dot{\mathbf{x}}_2 = f_2(\mathbf{x}_1, \mathbf{x}_2, \mathbf{x}_3, \mathbf{x}_4) + BM_M f_{Cl} \circ f_A(\mathbf{V}) \tag{26}$$

III. EXTENDED STATE OBSERVER

The equations (1) and (2) are built based on the 2D simulation data. However, the true flight environment is 3D cases where there is a notably wingtip vortex shedding phenomenon. It not only affects the lift coefficient, but also affects the improvement of lift coefficient by SJAs. What's more, it also changes the aerodynamic center of SJAs then affects l, brings the parameter uncertainties Δl in l. In the meantime, we do not know the exact value of the atmospheric moment coefficients m_x^*, m_y^* and m_z^*, too. The simplification of the equation (3) also brings uncertainties in function f_A. Similarly, there are uncertainties in function f_{Cl}, too. Due to there are parameter errors and model uncertainties, the f_2, B and M_M become unknown, which makes the control design complicated.

The ESO is not dependent on the exact mathematical model of the system, the disturbances, the unmodeled dynamics and the parameter uncertainties of the system are regarded as total uncertainty, and the total uncertainty is tracked and compensated in real time. Thus, it offering inherent robustness. Further, it is simple to implement. The observer takes the total uncertainty as an extended state of the system, hence, it is known as ESO.

In order to reduce the complicity of control design we take the unmodeled dynamics, parameter uncertainties and external disturbances existing in (10) together as the total uncertainty $\mathbf{d}(t)$, the new variable $\mathbf{d}(t)$ is defined as

$$\mathbf{d}(t) = f_2(\mathbf{x}_1, \mathbf{x}_2, \mathbf{x}_3, \mathbf{x}_4) + BM_M f_{Cl} \circ f_A(\mathbf{V}) - \hat{B}\hat{\mathbf{u}}(t). \tag{27}$$

Hence, system (10) can be rewritten as

$$\dot{\mathbf{x}}_2 = \mathbf{d}(t) + \hat{B}\hat{\mathbf{u}}(t), \tag{28}$$

where $\hat{B} = B^0 M_M^0$ is the estimation matrix coefficient, $\hat{\mathbf{u}}(t) = f_{Cl}^0 \circ f_A^0(\mathbf{V})$ is virtual control input. The matrix and functions $B^0, M_M^0, f_{Cl}^0, f_A^0$ are the corresponding nominal value, detailed in the section (V).

Next, we estimate the uncertainty $\mathbf{d}(t)$ as an extended state $\mathbf{x}_5(t)$ by a nonlinear continuous ESO. The second-order ESO has the following form

$$\begin{aligned} \mathbf{e} &= \mathbf{z}_1 - \mathbf{x}_2 \\ \dot{\mathbf{z}}_1 &= \mathbf{z}_2 - \beta_1\mathbf{e} + \hat{B}\hat{\mathbf{u}}(t) \\ \dot{\mathbf{z}}_2 &= -\beta_2\mathbf{fal}(\mathbf{e}, \lambda, \mu) \end{aligned} \tag{29}$$

where $\mathbf{z}_1, \mathbf{z}_2$ are the states of the observer, $\mathbf{e} = [e_1\ e_2\ e_3]^T$ is the estimation vector error between $\mathbf{z}_1$ and $\mathbf{x}_2$. β_1, β_2 are the observer gains rely on the time step Δt. $0 < \lambda < 1$, $\mu > 0$

are constant to be properly chosen. By choosing suitable parameters β_1, β_2, λ and μ, the error vector $\mathbf{e}$ will tend to 0, $\mathbf{z}_1 \to \mathbf{x}_2$ and $\mathbf{z}_2 \to \mathbf{d}(t)$. So the extended state $\mathbf{x}_5$ is obtained, $\mathbf{x}_5 = \mathbf{z}_2$. The function $\mathbf{fal}(\cdot, \cdot, \cdot)$ is defined as

$$\mathbf{fal}(\mathbf{e}, \lambda, \mu) = \begin{bmatrix} fal_1(e_1, \lambda, \mu) \\ fal_2(e_2, \lambda, \mu) \\ fal_3(e_3, \lambda, \mu) \end{bmatrix} \tag{30}$$

where

$$fal_i(e_i, \lambda, \mu) = \begin{cases} |e_i|^{\lambda}\ \mathrm{sgn}(e_i), |e_i| > \mu \\ e_i/\mu^{1-\lambda}, otherwise. \end{cases} \tag{31}$$

IV. CONTROLLER DESIGN

Due to the fact that the aircraft model is nonlinear in aerodynamics and there is a very complex nonlinear relation between the SJAs' excitation voltage and the lift/drag coefficient, a robust controller needs to be designed. As is well known, the SMC is robust to disturbances and unmodeled dynamics, especially for the control of nonlinear systems. It has attractive features to keep the system insensitive to uncertainties on sliding surfaces [27], [28]. Therefore, for solving the attitude tracking problem with parameter uncertainties, unmodeled dynamics and external disturbances exist in the aircraft system, a sliding-mode controller can be designed to force the state variables to converge to the reference states by compensating the total disturbances via the ESO. The objective is to design a feedback controller such that forcing the attitude angle $\mathbf{x}_1$ to track the given desired reference signal $\mathbf{x}_{1,r}$.

The tracking error of attitude angle is given as the following equation

$$\tilde{\mathbf{x}}_1 = \mathbf{x}_1 - \mathbf{x}_{1,r}. \tag{32}$$

The $\tilde{\mathbf{x}}_1 \to \mathbf{0}$ means that the attitude angle $\mathbf{x}_1$ have tracked the reference signal $\mathbf{x}_{1,r}$. Derivatives on both sides of the equation (32) are

$$\dot{\tilde{\mathbf{x}}}_1 = \dot{\mathbf{x}}_1 - \dot{\mathbf{x}}_{1,r} = f_1(\mathbf{x}_1)\mathbf{x}_2 - \dot{\mathbf{x}}_{1,r}. \tag{33}$$

Assuming that the aircraft angular velocity can be imposed instantaneously, define $\mathbf{x}_{2,r}$ as a virtual control input for the desired dynamics (34)

$$\dot{\tilde{\mathbf{x}}}_1 = -K_1\tilde{\mathbf{x}}_1 = -\begin{bmatrix} k_1 & 0 & 0 \\ 0 & k_2 & 0 \\ 0 & 0 & k_3 \end{bmatrix}\tilde{\mathbf{x}}_1. \tag{34}$$

Where, the design matrix K_1 is chosen as $k_1 > 0, k_2 > 0$, $k_3 > 0$ to ensure the asymptotic stability of (34). Combining equations (33) and (34), we can get the $\mathbf{x}_{2,r}$ as follows

$$\mathbf{x}_{2,r} = f_1^{-1}(\mathbf{x}_1)(\dot{\mathbf{x}}_{1,r} - K_1\tilde{\mathbf{x}}_1), \tag{35}$$

where, according to the assumption 2, we know that the $f_1(\mathbf{x}_1)$ is nonsingular. In order to guarantee the asymptotic stability of (34), a sliding controller is designed to achieve the above virtue control input $\mathbf{x}_{2,r}$.

The sliding surface is designed as following

$$\mathbf{S} = \mathbf{x}_2 - \mathbf{x}_{2,r}. \tag{36}$$

Derivative on both sides of the equation (36), and take replace the $\mathbf{d}(t)$ by $\mathbf{x}_5(t)$, we get the follow equation

$$\begin{aligned} \dot{\mathbf{S}} &= \dot{\mathbf{x}}_2 - \dot{\mathbf{x}}_{2,r} \\ &= \mathbf{x}_5(t) + \hat{B}\hat{\mathbf{u}}(t) - \dot{\mathbf{x}}_{2,r}. \end{aligned} \tag{37}$$

Taking the following reaching law

$$\dot{\mathbf{S}} = -\xi\mathbf{S} - \eta\mathrm{sig}(\mathbf{S})^r, \tag{38}$$

where $\xi = \mathrm{diag}[\xi_1, \xi_2, \xi_3], \eta = \mathrm{diag}[\eta_1, \eta_2, \eta_3]$, $\xi_i > 0$, $\eta_i > 0$ and $0 < r < 1$,

$$\mathrm{sig}(\mathbf{S})^r = [|S_1|^r\ \mathrm{sgn}(S_1), |S_2|^r \mathrm{sgn}(S_2), |S_3|^r\ \mathrm{sgn}(S_3)]^T. \tag{39}$$

Combine equations (37) and (38) we can give the control law

$$\hat{\mathbf{u}}(t) = \hat{B}^{\dagger}\ (-\xi\mathbf{S} - \eta\mathrm{sig}(\mathbf{S})^r - \mathbf{x}_5(t) + \dot{\mathbf{x}}_{2,r}) \tag{40}$$

where $\hat{B}^{\dagger} = \hat{B}^T(\hat{B}\hat{B}^T)^{-1}$ is the pseudo-inverse of $\hat{B}$.

V. RESULTS AND DISCUSSION

The control efficiency of the SJAs is best when wings' AOA is about 19 [deg], so we aim at maintaining wings' AOA about 19 [deg] by adjusting the attitude angle according to the path angle. In this paper, for simplification, we don't consider the actual path angle, as long as the aircraft's attitude angle equal to the reference attitude angle then the AOA is 19 [deg]. Numerical simulations were conducted to demonstrate the effectiveness of aircraft attitudes control using only SJAs.

Consider the aircraft model (4) and (5) with the nominal inertia matrix

$$I_0 = \begin{bmatrix} 3 & 0 & 2 \\ 0 & 4 & 0 \\ 2 & 0 & 5 \end{bmatrix} \mathrm{kg \cdot m^2} \tag{41}$$

and parameter uncertainties

$$\Delta I = \mathrm{diag}[0.5, 1, 1]\ \mathrm{kg \cdot m^2} \tag{42}$$

The above equation causes uncertainties in the rearranged moment inertias B, then $B = B^0 + \Delta B$.

The uncertainties of function f_2 partly caused by the equation (42) are expressed as Δ_1, and others caused by ΔU_{∞}, Δm_x^*, Δm_y^* and Δm_z^* taken together as Δ_2. So we can rewriter equation (14) as following

$$f_2 = f_2^0 + \Delta_1 + \Delta_2. \tag{43}$$

We also take account of the errors existing in equations (3) and (7), rewriter them as

$$f_V(V_i) = 0.67V_i + \Delta_3, \tag{44}$$

$$f_{Cd}(A_{SJ_i}) = -(k + \Delta k)f_{Cl}(A_{SJ_i}). \tag{45}$$

where $\Delta_3 = 0.1$, $\Delta k = 0.2$.

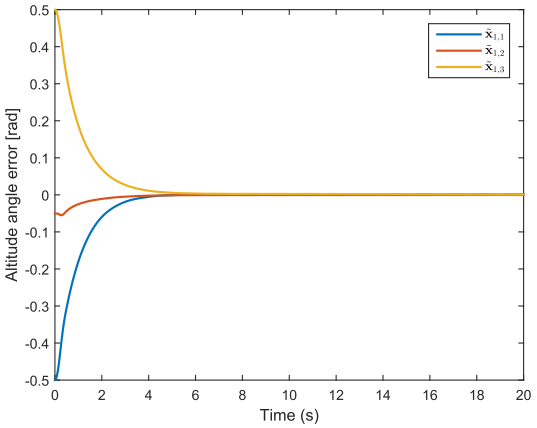

FIGURE 10. The attitude angle tracking errors.

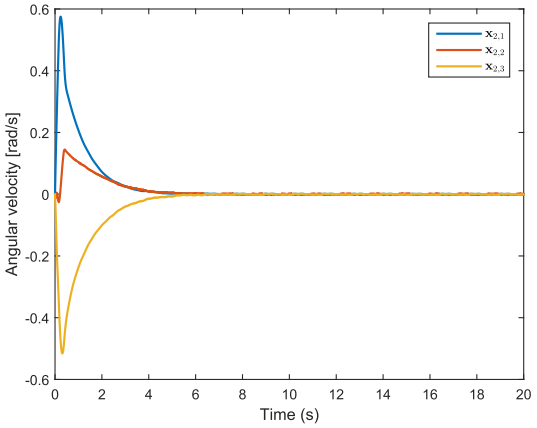

FIGURE 11. The angular velocity.

The nominal arm of force matrix l

$$l_0 = \begin{bmatrix} 0.5 & 0.5 & -1 & -1 \\ -0.8 & 0.8 & -0.4 & 0.4 \\ 0 & 0 & -0.01 & -0.01 \end{bmatrix} \text{kg} \cdot \text{m}^2 \quad (46)$$

and parameter uncertainties

$$\Delta l = -0.1l \quad (47)$$

The external disturbances are described as

$$\mathbf{D}(t) = \begin{bmatrix} 0.02\sin(5t) + 0.01\sin(15t) \\ 0.002\sin(10t) \\ 0.01\sin(0.2t) + 0.01\sin(20t) \end{bmatrix} \text{N} \cdot \text{m}. \quad (48)$$

The value of ESO parameters are $\beta_1 = 200, \beta_2 = 1600, \lambda = 0.5$ and $\mu = 0.1$, respectively. While, the gains of the system are $K = \text{diag}[1, 1, 1]$, $\xi = \text{diag}[10, 10, 10]$ and $\eta = \text{diag}[0.001, 0.001, 0.001]$, respectively.

The desired attitude angle of the numerical simulation, is given by

$$\mathbf{x}_{1,r} = \begin{bmatrix} 0.5 \\ 0.1 \\ -0.5 \end{bmatrix} \text{ rad / s}. \quad (49)$$

The initial value of attitude angle is $\mathbf{x}_1(0) = [0, 0.05, 0]^T$ rad and the initial value of the angular velocity is $\mathbf{x}_2(0) = [0, 0, 0]^T$ rad/s.

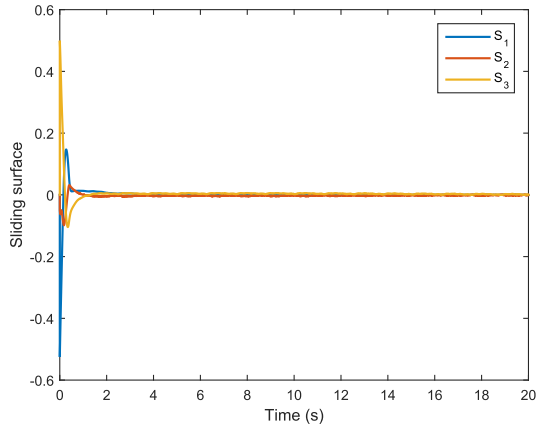

FIGURE 12. Sliding surface.

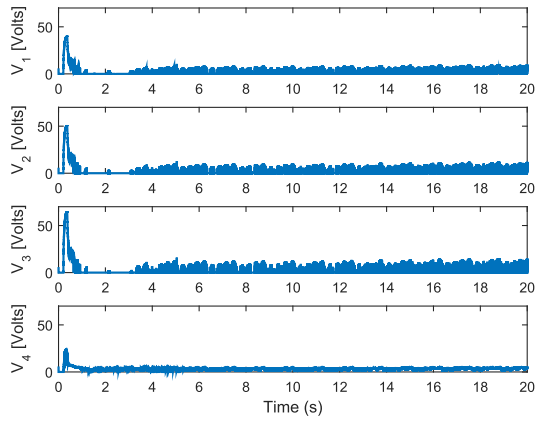

FIGURE 13. Voltage input of SJAs.

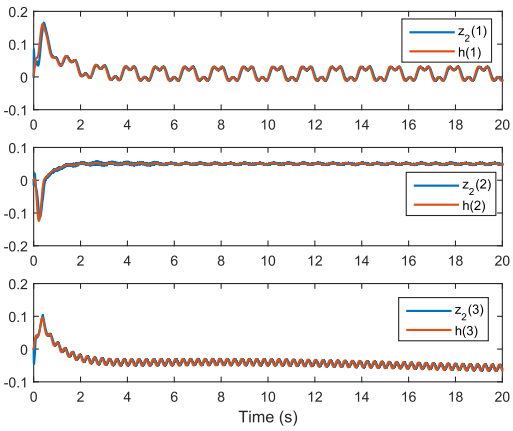

FIGURE 14. Estimation of disturbances via ESO.

Fig. 10 and Fig. 11 show the attitude angle tracking errors and angular velocity tracking errors, respectively. They prove that the sliding-mode controller is efficient to achieve attitude tracking when the parameter uncertainties, unmodeled dynamics and disturbances compensated by the ESO. The sliding surface is shown in Fig. 12 It is clear that the sliding mode is stable. Fig. 13 shows that the SJAs' voltage input control signals are high frequency oscillation. On the one hand, it can be suppressed by adjusting parameter K, ξ and η. On the other hand, benefit from SJAs' structural properties

the control signals is feasible, but it is infeasible to the conventional mechanical aileron and elevator. Fig. 14 shows the estimation of disturbances by ESO. Obviously, the estimated state $\mathbf{z}_2(t)$ converges to the total disturbance $\mathbf{d}(t)$ in finite time in spite of the parameter uncertainties, unmodeled dynamics and unknown external disturbances.

VI. CONCLUSION

In this paper, a novel active flow control technique is proposed to realize pitch-roll-yaw attitude control for a special aircraft at high AOA using only SJAs. Although the parameters uncertainties, unmodeled dynamics and unknown external disturbances exist the system, it has been proved that using only SJAs with a sliding mode controller based on ESO can effectively stabilize the aircraft at high AOA. Detailed simulation results have been presented to illustrate the developed method. The future of work, we will study on solely use only SJAs to achieve trajectory tracking control of UAV at a wide range of AOA and take the jet angle as a control input too.

REFERENCES

[1] L. Löfdahl and M. Gad-El-Hak, "MEMS applications in turbulence and flow control," *Prog. Aerosp. Sci.*, vol. 35, no. 2, pp. 101–203, 1999.

[2] D. Lockerby, "Numerical simulation of boundary-layer control using MEMS actuation," Ph.D. Dissertation, School Eng., The Univ. Warwick, Coventry, U.K., 2001. [Online]. Available: http://wrap.warwick.ac.uk/id/eprint/3076

[3] A. Huang, J. Lew, Y. Xu, Y.-C. Tai, and C.-M. Ho, "Microsensors and actuators for macrofluidic control," *IEEE Sensors J.*, vol. 4, no. 4, pp. 494–502, Aug. 2004.

[4] T. Yamagami, Y. Suzuki, and N. Kasagi, "Development of feedback control system of wall turbulence using MEMS devices," in *Proc. 6th Symp. Smart Control Turbulence*, 2005, pp. 135–141.

[5] M. Xiao, D. Changhui, and S. Shengxi, "A new phenomenon of acoustic streaming," *Acta Mechanica Sinica*, vol. 7, no. 3, pp. 193–198, 1991.

[6] A. Glezer and M. Amitay, "Synthetic jets," *Annu. Rev. Fluid Mech.*, vol. 34, no. 1, pp. 503–529, 1991, doi: 10.1146/annurev.fluid.34.090501.094913.

[7] M. Amitay *et al.*, "Control of internal flow separation using synthetic jet actuators," in *Proc. 38th Aerosp. Sci. Meeting Exhibit*, Reno, NV, USA, Jan. 2000, p. 903.

[8] M. Amitay, D. Smith, V. Kibens, D. Parekh, and A. Glezer, "Modification of the aerodynamics characteristics of an unconventional airfoil using synthetic jet actuators," *AIAA J.*, vol. 39, no. 3, pp. 361–370, 2001, doi: 10.2514/2.1323.

[9] D. Kral, F. Donovan, B. Cain, and W. Cary, "Numerical simulation of synthetic jet actuators," in *Proc. 4th Shear Flow Conf.*, Snowmass Villiage, CO, USA, 1997, p. 1824.

[10] M. Amitay, A. Honohan, M. Trautman, and A. Glezer, "Modification of the aerodynamic characteristics of bluff bodies using fluidic actuators," in *Proc. 28th AIAA Fluid Dyn. Conf.*, Snowmass Villiage, CO, USA, 1997, pp. 1997–2004.

[11] A. Seifert *et al.*, "Oscillatory blowing: A tool to delay boundary-layer separation," *AIAA J.*, vol. 31, no. 11, pp. 2052–2060, 1993.

[12] A. Glezer, "The formation of vortex rings," *Phys. Fluids*, vol. 31, no. 12, pp. 3532–3542, 1998.

[13] D. Neuburger and I. Wygnanski, "The use of vibrating ribbon to delay separation on twodimensional airfoils," in *Proc. Air Force Acad. Workshop Unsteady Separated Flow*, Colorado Springs, CO, USA, 1987, pp. 333–341.

[14] A. Bar-Sever, "Separation control on an airfoil by periodic forcing," *AIAA J.*, vol. 27, no. 6, pp. 820–821, 1989.

[15] S. Margalit, D. Greenblatt, A. Seifert, and I. Wygnanski, "Delta wing stall and roll control using segmented piezoelectric fluidic actuators," *J. Aircraft*, vol. 42, no. 3, pp. 698–709, 2005, doi: 10.2514/1.6904.

[16] A. Seifert, S. David, I. Fono, O. Stalnov, and I. Dayan, "Roll contrial via active flow control: From concept to flight," *J. Aircraft*, vol. 47, no. 3, pp. 864–874, 2010, doi: 10.2514/1.45910.

[17] C. Li and J. Yang, "The robust roll control using only synthetic jet actuators in high-angle-of-attack flight," in *Proc. IEEE 34th Chin. Control Conf. (CCC)*, Hangzhou, China, Jul. 2015, pp. 2865–2870, doi: 10.1109/ChiCC.2015.7260078.

[18] C. Li and J. Yang, "Roll control using only synthetic jet actuators at high angle of attack," *J. Aircraft*, vol. 54, no. 1, pp. 371–376, 2017.

[19] M. Ciuryla, M. Ciuryla, Y. Liu, J. Farnsworth, C. Kwan, and M. Amitay, "Flight control using synthetic jets on a Cessna 182 model," *J. Aircraft*, vol. 44, no. 2, pp. 642–653, 2007, doi: 10.2514/1.24961.

[20] J. Han, "From PID to active disturbance rejection control," *IEEE Trans. Ind. Electron.*, vol. 56, no. 3, pp. 900–906, Mar. 2009.

[21] S. Li, X. Yang, and D. Yang, "Active disturbance rejection control for high pointing accuracy and rotation speed," *Automatica*, vol. 45, no. 8, pp. 1854–1860, 2009.

[22] D. Sun, "Comments on active disturbance rejection control," *IEEE Trans. Ind. Electron.*, vol. 54, no. 6, pp. 3428–3429, Dec. 2007.

[23] Y. Xia, Z. Zhu, M. Fu, and S. Wang, "Attitude tracking of rigid spacecraft with bounded disturbances," *IEEE Trans. Ind. Electron.*, vol. 58, no. 2, pp. 647–659, Feb. 2011.

[24] Y. Xia, Z. Zhu, and M. Fu, "Back-stepping sliding mode control for missile systems based on extended state observer," *IET Control Theory Appl.*, vol. 5, no. 1, pp. 93–102, 2011.

[25] C. Li and J. Yang, "Flight control using only synthetic jet actuators in high-angle-of-attack," in *Proc. IEEE 35th Chin. Control Conf. (CCC)*, Chengdu, China, Jul. 2016, pp. 10662–10667, doi: 10.1109/ChiCC.2016.7555047.

[26] S. David and A. Seifert, "On the generation of yawing moment using active flow control," *Int. J. Heat Fluid Flow*, vol. 38, pp. 72–81, Dec. 2012.

[27] W. Gao and J. C. Hung, "Variable structure control of nonlinear systems: A new approach," *IEEE Trans. Ind. Electron.*, vol. 40, no. 1, pp. 45–55, Feb. 1993.

[28] M. Mahmoud, E. Boukas, and A. Ismail, "Robust adaptive control of uncertain discrete-time state-delay systems," *Comput. Math. Appl.*, vol. 55, no. 12, pp. 2887–2908, 2008.

CHUNZHI LI received the B.S. degree from the School of Mathematics, Jilin University, Changchun, China, in 2009. He is currently pursuing the Ph.D. degree with the Department of Mechanics and Engineering Science, Peking University, Beijing, China. His major research interests include flight dynamics and control and active flow control.

TINGTING ZHANG received the B.S. degree from the Nanjing University of Aeronautics and Astronautics, Nanjing, China, in 2016. She is currently pursuing the M.S. degree with the Department of Mechanics and Engineering Science, Peking University, Beijing, China. Her major research interests include flight dynamics and control, and network control system.

JIANYING YANG received the B.S. degree from the Department of Aerospace, Northwestern Polytechnical University, Xian, China, in 1988, and the Ph.D. degree from the Beijing institute of technology, Beijing, China. His major research interests include modern control theory, flight mechanics, aircraft navigation, control and guidance, advanced control technology of complex high-speed mobile movement, key scientific problems of high-speed flight dynamics and control in the near space, and satellite orbital maneuvering control technology.